Journal of Nuclear and Particle Physics 2013, 3(4): 121-125
DOI: 10.5923/j.jnpp.20130304.09

Plasma Internal Inductance in Presence of Toroidal Field Ripple of Tokamak

A. Salar Elahi*, M. Ghoranneviss

Plasma Physics Research Center, Science and Research Branch, Islamic Azad University, Tehran, Iran

Abstract In this research we investigated the effects of toroidal field ripple of tokamak on the plasma internal inductance. For this purpose, array of magnetic probes and also a diamagnetic loop with its compensation coil were designed, constructed, and installed on outer surface of the IR-T1 tokamak. Amplitude of the TF ripple is obtained 0.01, and also the effect of the TF ripple on the plasma internal inductance was discussed. In the high field side region of tokamak chamber, the TF ripple effect is increasing of the plasma internal inductance, whereas the low field side has inverse situation.

Keywords Tokamak, Toroidal Field Ripple, Plasma Internal Inductance

1. Introduction

Usually tokamaks plasma equilibria are investigated as two-dimensional (axisymmetric) systems. Although this symmetry offers many advantages for its analysis, but realistic tokamaks consists of finite number of Toroidal Field (TF) coils. Then, this discreteness yields the toroidal field ripples (a periodic variation of the toroidal magnetic field). In other words, realistic tokamaks could not be axisymmetric configurations. Most of the TF ripple studies have been done on effects of the TF ripple on confinement of the high energy alpha particles, formation of internal transport barriers, plasma rotation, and H-mode performance. In IR-T1 Tokamak, which is a small, low Beta and large aspect ratio tokamak with a circular cross section (see Table 1), the number N of TF coils is 16, and then the period of the TF ripple was 22.5°. In this paper we present the effects of the TF ripple on the plasma internal inductance in IR-T1 tokamak. Determination of the internal inductance is essential for tokamak experiments and optimized operation. Also some of the plasma information can be deduced from this parameter, such as plasma toroidal current profile.

Magnetic diagnostics, in particular diamagnetic loop (toroidal flux loop) are commonly used in tokamaks to measure the variation of toroidal flux induced by the plasma and then the poloidal Beta. On the other hand, the magnetic fields distribution outside the plasma provides the measurement of the combination of poloidal Beta and internal inductance, via the Shafranov parameter (Λ). Then measurement of Λ from the magnetic probes and poloidal Beta from diamagnetic loop gives a value of internal inductance[1-65]. In this paper we present experimental investigation of the TF ripple on this parameter. Because of dependence of the toroidal field on the TF ripple amplitude, therefore we expect that this parameter is also depending on TF ripple amplitude. Brief approach for determinations of the TF ripple and Shafranov parameter using the discrete magnetic probes will be present in section 2. Diamagnetic loop method for measurement of the poloidal Beta and internal inductance will present in section 3. Experimental results of effects of TF ripple on the plasma internal inductance will discuss in section 4. Summary and discussion will present in section 5.

Table 1. Main Parameters of the IR-T1 Tokamak

Parameters	Value
Major Radius	45 cm
Minor Radius	12.5 cm
Toroidal Field	〈 1.0 T
Plasma Current	〈 40 kA
Discharge Duration	〈 35 ms
Electron Density	$0.7\text{-}1.5\times 10^{13}\ \mathrm{cm}^{-3}$
Toroidal Field Coils	16

2. Determinations of the TF Ripple and Shafranov Parameter Using the Discrete Magnetic Probes

A simple analytic model of the toroidal magnetic field strength widely used in the analysis is[1]:

$$B_\phi(\theta,\phi) = B_0\left(1-\varepsilon\cos\theta - \delta\cos N\phi\right), \qquad (1)$$

* Corresponding author:
Salari_phy@yahoo.com (A. Salar Elahi)
Published online at http://journal.sapub.org/jnpp

where B_0 is the toroidal magnetic field at center of the tokamak chamber, θ and ϕ are poloidal and toroidal angles respectively, ε is the inverse aspect ratio, N is the number of the toroidal field coils, and δ is the amplitude of the TF ripple where defined as:

$$\delta = \frac{\delta B}{\langle B \rangle_\phi} \approx \frac{B_{\max} - B_{\min}}{B_{\max} + B_{\min}}. \quad (2)$$

In the IR-T1 the number of TF coils is 16, then the period of the TF ripple was 22.5°, and the inverse aspect ratio is 0.278. From the Eq. (1) we can write:

$$\delta = \frac{1}{4}\left(\frac{B_\phi(\theta=0,\phi=\pi/N) - B_\phi(\theta=0,\phi=0)}{B_0}\right) + \frac{1}{4}\left(\frac{B_\phi(\theta=\pi,\phi=\pi/N) - B_\phi(\theta=\pi,\phi=0)}{B_0}\right), \quad (3)$$

where these values of the toroidal magnetic fields can be determined using the magnetic probes at above poloidal and toroidal angles. Our measurements show that the amplitude of the TF ripple in IR-T1 is 0.01, as shown in Fig. (1).

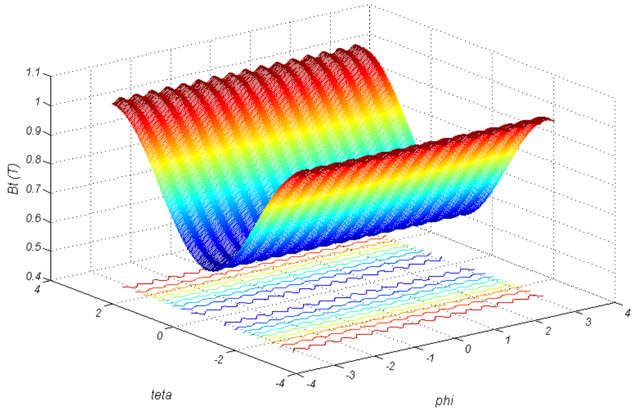

Figure (1). Dependence of the Toroidal Magnetic Field on the Poloidal and Toroidal Angles, TF Ripple is also observable

Also the Shafranov parameter relate to the distribution of magnetic fields around the plasma current. Therefore, those can be written in terms of the tangential and normal components of the magnetic field on the contour Γ (see Fig. (2)). Distributions of the tangential and normal magnetic fields are also can be written in the first order of the inverse aspect ratio as follows, respectively[2,3,5]:

$$B_\theta = \frac{\mu_0 I_p}{2\pi b} - \frac{\mu_0 I_p}{4\pi R_0} \times \left\{\ln\frac{a}{b} + 1 - \left(\Lambda + \frac{1}{2}\right)\left(\frac{a^2}{b^2} + 1\right) - \frac{2R_0\Delta_s}{b^2}\right\}\cos\theta, \quad (4)$$

$$B_\rho = -\frac{\mu_0 I_p}{4\pi R_0} \times \left\{\ln\frac{a}{b} + \left(\Lambda + \frac{1}{2}\right)\left(\frac{a^2}{b^2} - 1\right) + \frac{2R_0\Delta_s}{b^2}\right\}\sin\theta \quad (5)$$

where R_0 is the major radius of the vacuum vessel, Δ_s is the Shafranov shift, I_p is the plasma current, a and b are the minor plasma radius and minor chamber radius respectively. These equations accurate for low β plasma, large aspect ratio, and circular cross section tokamaks as IR-T1, and where:

$$\Lambda = \beta_p + l_i/2 - 1 = \ln\frac{a}{b} + \frac{\pi R_0}{\mu_0 I_p}(\langle B_\theta \rangle + \langle B_\rho \rangle), \quad (6)$$

where

$$\langle B_\theta \rangle = B_\theta(\theta = 0) - B_\theta(\theta = \pi),$$
$$\langle B_\rho \rangle = B_\rho(\theta = \frac{\pi}{2}) - B_\rho(\theta = \frac{3\pi}{2}), \quad (7)$$

and where β_p is the poloidal Beta and l_i is the plasma internal inductance. We can obtain B_θ and B_ρ after compensating and integrating of output signals of the magnetic probes. The compensation done by fields discharge without plasma and receives output signals of the magnetic probes and subtract those from total output signals. Experimental results will present in the section 4.

3. Determination of the Plasma Internal Inductance Using the Diamagnetic Loop

The toroidal flux that produced by the plasma is related to the total perpendicular thermal energy of the plasma. This diamagnetic flux is usually measured with the diamagnetic loop. In cases of the ohmically heated tokamaks (low beta) where the plasma energy density is small compared to the energy density of the magnetic field, the change in the total toroidal magnetic flux is small. Therefore a reference signal equal to the vacuum toroidal magnetic flux is usually subtracted from it, giving a net toroidal flux equal to the diamagnetic flux $\Delta\Phi_D$ produced by the circular plasma. Relation between the diamagnetic flux and the poloidal beta derived from simplified equilibrium relation[2-7]:

$$\Delta\Phi_D = \Phi_{total} - \Phi_{vacuum} \approx \frac{\mu_0^2 I_p^2}{8\pi B_\phi}\left(1 - \beta_p\right), \quad (8)$$

by substituting the Eq. (1) in the Eq. (8) we have:

$$\beta_p = 1 - \frac{8\pi B_0(1 - \varepsilon\cos\theta - \delta\cos N\phi)}{\mu_0^2 I_p^2}\Delta\Phi_D, \quad (9)$$

where $\Phi_{vacuum} = \Phi_T + \Phi_O + \Phi_V + \Phi_E$, and where B_0 is the toroidal magnetic field in the absence of the plasma which can be obtained by the magnetic probe, I_p is the plasma current which can be obtained by the Rogowski coil, Φ_T is the toroidal flux because of toroidal field coils,

Φ_O and Φ_V are the passing flux through loop due to possible misalignment between ohmic field and vertical field and the diamagnetic loop, and Φ_E is the toroidal field due to eddy current on the vacuum chamber. These fluxes can be compensated either with compensation coil or fields discharge without plasma. It must be noted that compensating coil for diamagnetic loop is wrapped out of the plasma current, and only the toroidal flux (which is induced by the change of toroidal field coil current when plasma discharges) can be received. So the diamagnetic flux $\Delta\Phi_D$ caused by plasma current can be measured from the diamagnetic and compensating coil using subtraction. Therefore, according to above two sections we can find the internal inductance. From Eq. (6) we have:

$$li = 2(\Lambda - \beta_p + 1) \tag{10}$$

By substituting the Eq. (6) and (9) in Eq. (10), we can write:

$$li = 2\ln\frac{a}{b} + \frac{2\pi R_0}{\mu_0 I_p}(\langle B_\theta\rangle + \langle B_\rho\rangle) + \frac{16\pi B_0(1-\varepsilon\cos\theta - \delta\cos N\phi)}{\mu_0^2 I_p^2}\Delta\Phi_D, \tag{11}$$

where the effect of the TF ripple introduced in the Shafranov parameter.

Experimental results of effects of the TF ripple on the internal inductance will present in next section.

4. Experimental Results

According to above discussion, we determined the plasma internal inductance and the effects of TF ripple on it. Results present in Figs. (2) and (3). As shown, the difference between the internal inductance in presence of the TF ripple and in absence of the TF ripple is in order of the 10^{-2}, and in the high field side region of tokamak chamber, the TF ripple effect is increasing of the plasma internal inductance, whereas the low field side has inverse situation.

5. Summary and Discussion

In this research we investigated the effects of TF ripple on the plasma internal inductance in IR-T1 Tokamak. For this purpose, array of magnetic probes and also a diamagnetic loop with its compensation coil were designed, constructed, and installed on the outer surface of the IR-T1. Amplitude of the TF ripple is obtained 0.01, and also the effects of the TF ripple on the plasma internal inductance presented. One of the results is that the difference between the internal inductance in presence of the TF ripple and in absence of the TF ripple is in order of the 10^{-2}, and also in the high field side region the difference is positive, whereas in low field side the difference is negative. In other words, in the high field side region of tokamak chamber, the TF ripple effect is increasing of the plasma internal inductance, whereas the low field side has inverse situation.

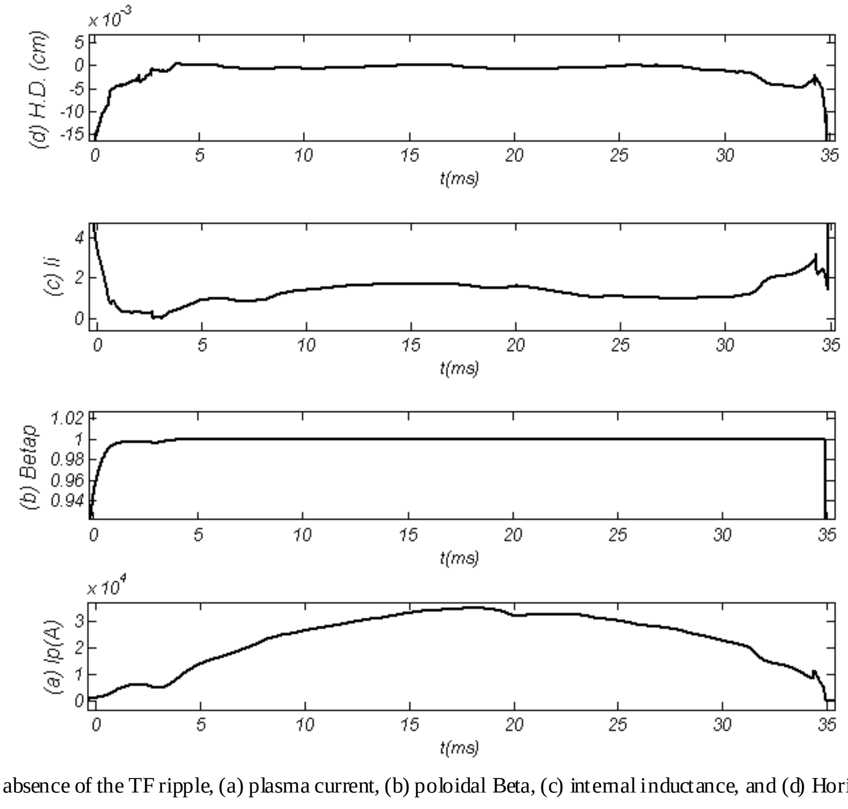

Figure (2). Parameters in absence of the TF ripple, (a) plasma current, (b) poloidal Beta, (c) internal inductance, and (d) Horizontal Displacement (H.D.)

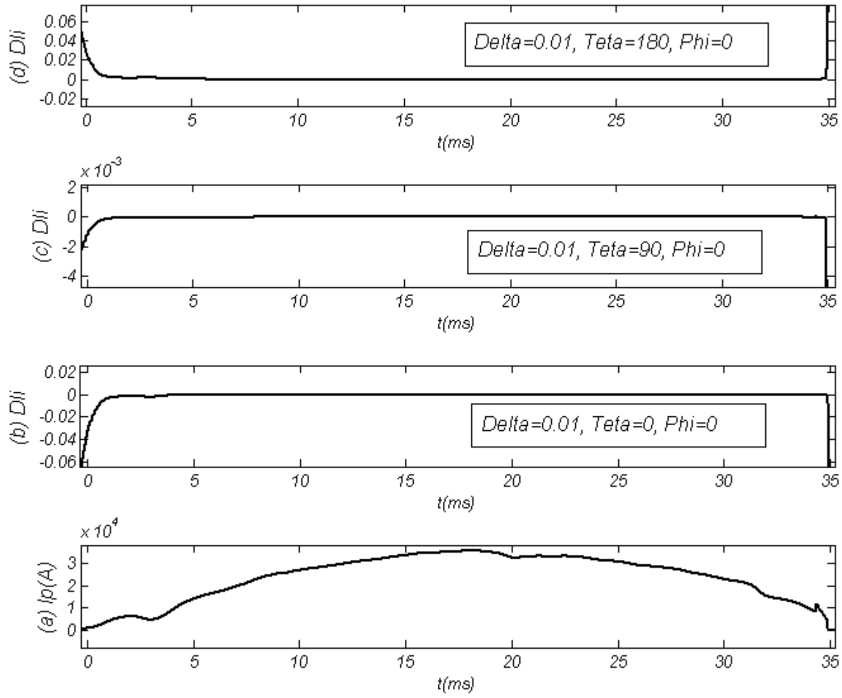

Figure (3). Effects of the TF ripple amplitude on the difference of internal inductance with and without TF ripple (Dli) at different poloidal angles. As shown, difference between the internal inductance in present of the TF ripple and in absent of the TF ripple is in order of the 10^{-2} . Also in the high field side region ($\theta = 180^o$) the difference is positive, but in low field side ($\theta = 0^o$) the difference is negative

REFERENCES

[1] K. Nakamura and M. Ghoranneviss, Fusion Eng. Des. 66-68 (2003) 771-777.

[2] V. S. Mukhovatov and V. D. Shafranov, Nucl. Fusion 11, (1971), 605

[3] I. P. Shkarofsky, Phys. Fluids 25 (1) 89-96, (1982).

[4] G.S. Lee and and M. Ghoranneviss, Nucl. Fusion 41, 1515 (2001)

[5] S.H. Seo, Phys. Plasmas 16, 032501 (2009)

[6] A. Salar Elahi and M. Ghoranneviss, IEEE Trans. Plasma Science 38 (2), 181-185, (2010)

[7] A. Salar Elahi and M. Ghoranneviss, IEEE Trans. Plasma Science 38 (9), 3163-3167, (2010)

[8] A. Salar Elahi and M. Ghoranneviss, J. Plasma Physics 76 (1), 1-8, (2009)

[9] A. Salar Elahi and M. Ghoranneviss, Fusion Engineering and Design 85, 724–727, (2010)

[10] A. Salar Elahi and M. Ghoranneviss, Phys. Scripta 80, 045501, (2009)

[11] A. Salar Elahi and M. Ghoranneviss, Phys. Scripta 80, 055502, (2009)

[12] A. Salar Elahi and M. Ghoranneviss, Phys. Scripta 81 (5), 055501, (2010)

[13] A. Salar Elahi and M. Ghoranneviss, Phys. Scripta 82, 025502, (2010)

[14] M. Ghoranneviss, A. Salar Elahi, Phys. Scripta 82 (3), 035502, (2010)

[15] A. Salar Elahi and M. Ghoranneviss, J. Fusion Energy 28 (4), 346-349, (2009)

[16] A. Salar Elahi and M. Ghoranneviss, J. Fusion Energy 28 (4), 416-419, (2009)

[17] A. Salar Elahi and M. Ghoranneviss, J. Fusion Energy 28 (4), 408-411, (2009)

[18] A. Salar Elahi and M. Ghoranneviss, J. Fusion Energy 28 (4), 412-415, (2009)

[19] A. Salar Elahi and M. Ghoranneviss, J. Fusion Energy 28 (4), 394-397, (2009)

[20] A. Salar Elahi and M. Ghoranneviss, J. Fusion Energy 28 (4), 404-407, (2009)

[21] A. Salar Elahi and M. Ghoranneviss, J. Fusion Energy 28 (4), 390-393, (2009)

[22] A. Salar Elahi and M. Ghoranneviss, J. Fusion Energy 28 (4), 385-389, (2009)

[23] A. Rahimi Rad, M. Ghoranneviss, M. Emami, and A. Salar Elahi, J. Fusion Energy 28 (4), 420-426, (2009)

[24] A. Salar Elahi and M. Ghoranneviss, J. Fusion Energy 29 (1), 1-4, (2010)

[25] A. Salar Elahi and M. Ghoranneviss, J. Fusion Energy 29 (1), 22-25, (2010)

[26] A. Salar Elahi and M. Ghoranneviss, J. Fusion Energy 29 (1), 29-31, (2010)

[27] A. Salar Elahi and M. Ghoranneviss, J. Fusion Energy 29 (1), 26-28, (2010)

[28] A. Salar Elahi and M. Ghoranneviss, J. Fusion Energy 29 (1), 32-35, (2010)

[29] A. Salar Elahi and M. Ghoranneviss, J. Fusion Energy 29 (1), 36-40, (2010)

[30] A. Salar Elahi and M. Ghoranneviss, J. Fusion Energy 29 (1), 62-64, (2010)

[31] A. Salar Elahi and M. Ghoranneviss, J. Fusion Energy 29 (1), 76-82, (2010)

[32] A. Rahimi Rad, M. Emami, M. Ghoranneviss, A. Salar Elahi, J. Fusion Energy 29 (1), 73-75, (2010)

[33] A. Salar Elahi and M. Ghoranneviss, J. Fusion Energy 29 (1), 83-87, (2010)

[34] A. Salar Elahi and M. Ghoranneviss, J. Fusion Energy 29 (1), 88-93, (2010)

[35] A. Salar Elahi and M. Ghoranneviss, J. Fusion Energy 29 (3), 209-214, (2010)

[36] A. Salar Elahi and M. Ghoranneviss, J. Fusion Energy 29 (3), 232-236, (2010)

[37] A. Salar Elahi and M. Ghoranneviss, J. Fusion Energy 29 (3), 251-255, (2010)

[38] A. Salar Elahi and M. Ghoranneviss, J. Fusion Energy 29 (3), 279-284, (2010)

[39] M. Ghoranneviss, A. Salar Elahi, J. Fusion Energy 29 (5), 467-470, (2010)

[40] A. Salar Elahi and M. Ghoranneviss, J. Fusion Energy 29 (5), 461-465, (2010)

[41] A. Salar Elahi and M. Ghoranneviss, Brazilian J. Physics 40 (3), 323-326, (2010)

[42] A. Salar Elahi and M. Ghoranneviss, J. Fusion Energy 30 (2), 116-120, (2011)

[43] M.R. Ghanbari, M. Ghoranneviss, A. Salar Elahi, Phys. Scripta 83, 055501, (2011)

[44] A. Salar Elahi, J. Fusion Energy 30 (6), 477-480, (2011), 477-480

[45] A. Salar Elahi and M. Ghoranneviss, Fusion Engineering and Design 86, 442–445, (2011)

[46] A. Salar Elahi and M. Ghoranneviss, J. Fusion Energy 31 (2), 191-194, (2012)

[47] M.R. Ghanbari, M. Ghoranneviss, A. Salar Elahi, R. Arvin and S. Mohammadi, Radiation Effects & Defects in Solids 166 (10), 789–794, (2011)

[48] A. Salar Elahi and M. Ghoranneviss, IEEE Trans. Plasma Science 40 (3), 892-897, (2012)

[49] Z. Goodarzi, M. Ghoranneviss and A. Salar Elahi, J. Fusion Energy 32 (1), 103-106, (2013)

[50] M.R. Ghanbari, M. Ghoranneviss, A. Salar Elahi, Phys. Scripta 85 (5), 055502, (2012)

[51] A. Salar Elahi and M. Ghoranneviss, Radiation Effects and Defects in Solids 168(1), 42-47, (2013)

[52] K. Mikaili Agah, M. Ghoranneviss, A. Salar Elahi, J. Fusion Energy 32 (2), 268-272, (2013)

[53] A. Salar Elahi and M. Ghoranneviss, Fusion Engineering and Design 88 (2), 94-99, (2013)

[54] A. Salar Elahi and M. Ghoranneviss, IEEE Transactions on Plasma Science 41 (2), 334-340, (2013)

[55] A. Salar Elahi and M. Ghoranneviss, J. of Fusion Energy 32, 496-502, (2013)

[56] A. Salar Elahi and M. Ghoranneviss, Review of Scientific Instruments 84 (5), 053504 (2013)

[57] A. Salar Elahi and M. Ghoranneviss, J. Nuclear and Particle Physics 1(1), 10-15, (2011)

[58] A. Salar Elahi and M. Ghoranneviss, J. Nuclear and Particle Physics 2(2), 1-5, (2012)

[59] A. Salar Elahi and M. Ghoranneviss, J. Nuclear and Particle Physics 2(2), 22-25, (2012)

[60] A. Salar Elahi and M. Ghoranneviss, J. Nuclear and Particle Physics 2(4), 91-97, (2012)

[61] A. Salar Elahi and M. Ghoranneviss, J. Nuclear and Particle Physics 2(4), 101-106, (2012)

[62] A. Salar Elahi and M. Ghoranneviss, J. Nuclear and Particle Physics 2(5), 112-118, (2012)

[63] A. Salar Elahi and M. Ghoranneviss, J. Nuclear and Particle Physics 2(6), 142-146, (2012)

[64] A. Salar Elahi and M. Ghoranneviss, J. Nuclear and Particle Physics 3(1), 1-7, (2013)

[65] A. Salar Elahi and M. Ghoranneviss, J. Nuclear and Particle Physics 3(1), 14-19, (2013)